

## Model of electron-hole droplet condensation in semiconductors

T. L. Reinecke

*Naval Research Laboratory, Washington, D. C. 20375*

M. C. Lega and S. C. Ying

*Department of Physics, Brown University, Providence, Rhode Island 02912*

(Received 4 April 1979)

The phase diagram for electron-hole droplet condensation is addressed, and detailed calculations are given for the elemental systems Ge and Si with varying uniaxial strain which have properties that vary systematically over relatively wide ranges. A model based on noninteracting droplet fluctuations is used to describe the phase diagram. This model expresses the liquid and gas densities in terms of properties of the low-temperature liquid phase, most notably its surface tension. Detailed microscopic calculations based on a gradient expansion of the free energy are given for the temperature-dependent surface tension of droplets in six model systems involving Ge and Si with uniaxial strain; these are zero strain, intermediate strain sufficient to remove the electron-band degeneracy, and large strain which also removes the hole-band degeneracy. Phase diagrams are given for these systems and show changes corresponding to the systematic decrease in the electron-hole droplet binding energy with increasing uniaxial strain. The resulting critical temperatures and densities are compared to the results of new calculations based on the uniform plasma approach to the critical point. The phase diagrams, including the values of the critical parameters, are in good agreement with experiment for unstressed Ge and Si and for Ge with fairly large uniaxial stress. The model provides a parameter which characterizes the shape of the phase diagram, and systematic changes in shape with strain are obtained.

### I. INTRODUCTION

At low temperatures and fairly high density, electrons and holes in many semiconductor systems undergo a liquid-gas-like condensation into micron sized droplets of "metallic" electron-hole liquid (EHL). In recent years this phenomenon has received much experimental<sup>1</sup> and theoretical<sup>2</sup> study. Because the effective-mass approximation accounts in detail for the electron-lattice (ion) interaction in most semiconductors and the band-structure parameters are known very accurately in these systems, the electron-hole droplet (EHD) system offers perhaps the best testing ground presently known for the understanding of the effects (on both bulk and surface properties) of electron-electron interactions which play an important role in many aspects of solid-state physics. In addition EHD condensation is unusual among phase transitions in that it is the most quantum of known transitions; in it the electronic system remains largely degenerate up to the critical temperature.

EHD condensation has received the most detailed investigation in the indirect gap, elemental semiconductors Ge and Si, but it has also been studied in other systems notably Ge and Si with uniaxial stress,<sup>3-5</sup> especially so quite recently,<sup>6-10</sup> and also in

compound semiconductors. The existence of EHD condensation in a particular semiconductor system and the properties of the resulting condensate are known to depend sensitively on the band structure of the semiconductor. The ground-state energetics of EHL are understood quite well especially in Ge and Si. At zero temperature the ground-state energy of EHL is composed of kinetic energy, exchange energy, and correlation energy. Ge and Si have respectively four- and sixfold degenerate electron conduction bands and coupled heavy and light hole bands. The degeneracy (and anisotropy) of the bands plays an important role in reducing the EHL ground-state energy below that of the exciton, thereby stabilizing the EHL mainly by reducing the kinetic energy.

As the number of systems in which EHD condensation is observed increases and becomes more varied, the systematics of this condensation is coming to be of considerable interest. It is in part the purpose of the present work to study the systematic changes in the properties of the condensation in a set of well characterized systems with widely varying energetics. Ge and Si with varying uniaxial strain along the [111] and [100] directions, respectively, constitute an attractive set of systems for such a study in that their band structure is known well, and detailed

calculations are available for the correlation energies. Under moderate strain one electron valley in Ge and two in Si are lowered with respect to the others thus lifting the conduction-band degeneracy; with still larger uniaxial strain the hole-band degeneracy is also lifted. These are the six model systems to be studied in detail here. As the band degeneracy decreases with increasing strain the kinetic energy increases, and the binding energy of the EHL relative to the exciton decreases; for example, for unstrained Ge the EHL is bound strongly, but for Ge with large strain the binding is weak.<sup>7-9</sup>

The full temperature-dependent phase transition for temperatures up to the critical temperature  $T_c$  is less well understood than the ground-state energetics. The most complete picture of the phase transition is provided by the phase diagram (see Fig. 1), which is a boundary (in density  $\rho$  and temperature  $T$ ) separating a phase composed of a low-density "gas" of excitons, electrons, and holes from a phase of high-density "metallic" liquid (EHL) and from a two phase region involving their coexistence which is characterized by electron-hole droplets (EHD). The shapes of both sides of the phase diagram for  $T < \frac{1}{2}T_c$  are understood reasonably well on the basis of quite simple arguments: On the gas side of  $T < \frac{1}{2}T_c$  ( $\rho < 2 \times 10^{15} \text{ cm}^{-3}$  for Ge) the exponential dependence of the density on  $T$  is given by thermal equilibrium between a noninteracting classical gas and the liquid phase.<sup>1</sup> On the liquid side for  $T < \frac{1}{2}T_c$ , the  $T^2$  dependence of the density can be understood with a simple picture of noninteracting degenerate fermions.<sup>1,2,11</sup> For

$T \geq \frac{1}{2}T_c$  however these simple descriptions fail, and there results a flattening of the top of the phase diagram (see Fig. 1).

Theoretical understanding of the phase diagram in the region  $T \geq \frac{1}{2}T_c$  is hampered by an inadequate knowledge of the energetics of the electron-hole system. In the intermediate density region, between the dense electron-hole system and the low-density excitons, the effects of multiple scattering between electrons and holes become increasingly important, and existing many-body theories do not provide an adequate description of the exchange-correlation energy in this region. Furthermore, as  $T$  approaches  $T_c$ , critical fluctuations become increasingly important, and these fluctuation contributions to the free energy also have not been calculated from a microscopic theory.

Often in discussing experimental data, it has simply been suggested that the scaled phase diagram in this region has the same shape as that for classical gas condensation.<sup>1,7,12</sup> Among theoretical approaches, Droz and Combescot<sup>13</sup> have suggested a parameterized lattice-gas model. Reinecke and Ying<sup>14</sup> introduced a model based on droplet fluctuations. Mahler and Birman<sup>15</sup> have made model approximations for the constituents and energetics for the intermediate density regime.

In the present paper the droplet fluctuation model is discussed fully, and it is used to treat in detail EHD condensation in Ge and Si with varying uniaxial strain. This model expresses the densities in terms of the properties of the low-temperature liquid phase, most notably its surface tension. Detailed microscopic calculations are made of the temperature-dependent surface tension for the six systems given by Ge and Si with zero, intermediate, and large uniaxial strain, and the corresponding phase diagrams are given. These results furnish perhaps the most complete picture to date of the systematic behavior of EHD condensation in a set of systems with widely varying energetics. Brief accounts of some aspects of the droplet fluctuation model for EHD condensation have appeared previously.<sup>14,16,17</sup> It is the purpose of the present paper to give a fairly complete account of the model including comparison with experiment and with other calculations and also to discuss in some detail its application to the set of strained elemental systems.

The paper is organized as follows: The droplet fluctuation model is developed in Sec. II A. Calculations of the temperature-dependent surface tension are given in Sec. II B, and the phase diagrams for the six model systems are given in Sec. II C. These results are compared with experiment in Sec. III A. The resulting critical points are compared with new evaluations of the critical points of these systems using the uniform plasma-model description of the system in Sec. III B. The shapes of the phase diagrams are discussed in Sec. III C.

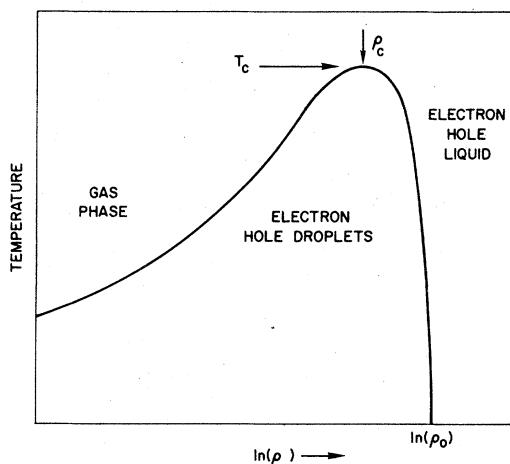


FIG. 1. Schematic representation of typical phase diagram for electron-hole droplet condensation in units of  $\ln$  of density vs temperature.

## II. DROPLET FLUCTUATION MODEL AND CALCULATIONS

### A. Droplet fluctuation model for electron-hole droplet condensation in semiconductors

In order to describe the phase diagram for  $T \geq \frac{1}{2}T_c$ , we employ a simple, physically clear model<sup>14</sup> based on the concept of droplet fluctuations. This model is an extension of a model already used to discuss the condensation of classical gases<sup>18</sup> and used more recently to discuss certain aspects of critical phenomena.<sup>19</sup> In this model the gas near the condensation curve is pictured as containing a distribution of noninteracting dropletlike fluctuations at constant chemical potential  $\mu$  and temperature  $T$ . Then the gas density is given by

$$\rho_G = q_0 \sum_{n=1}^{\infty} n \exp\{-[F_B n + \sigma a n^\eta + k_B T \tau \ln(n) - \mu n]/k_B T\} \quad (1)$$

Here the free energy of a droplet fluctuation of  $n$  electron-hole pairs<sup>20</sup> is separated into a bulk term  $F_B n$  where  $F_B$  is the bulk free energy per pair, a surface term  $\sigma a n^\eta$ , where  $\sigma$  is a surface tension parameter for the fluctuation, and  $a n^\eta$  is the surface area, and a higher-order term in  $\ln(n)$ <sup>21</sup>;  $q_0$  is an overall proportionality constant.

The condensation point and the critical point are determined as follows. The exponential factor Eq. (1) gives the probability of a fluctuation of  $n$  pairs. For  $F_B < \mu$  the probability of very large fluctuations diverges, whereas for  $F_B > \mu$  it does not. Thus the condition  $\mu = F_B(T)$  indicates the onset of a stable liquid phase and gives the condensation point. Using this condition the gas density on the coexistence curve is

$$\rho_{G, \text{coex.}} = q_0 \sum_{n=1}^{\infty} n^{1-\tau} \exp\left[-\frac{\sigma(T) a n^\eta}{k_B T}\right] \quad (2)$$

As  $T$  approaches  $T_c$  the surface tension parameter  $\sigma(T)$  decreases, and fluctuations increase. Finally at a temperature for which  $\sigma(T)$  vanishes, stable droplet formation is no longer possible, and thus the condition

$$\sigma(T = T_c) = 0 \quad (3)$$

determines  $T_c$ .

In a manner similar to Eq. (1) we picture the liquid phase near the condensation curve as dense EHL containing "bubble"-like fluctuations of the gas. On the liquid side of the coexistence curve ( $\mu = F_B$ ) the density is then

$$\rho_{L, \text{coex.}} = \rho_0(T) - q_0 \sum_{n=1}^{\infty} n^{1-\tau} \exp\left[-\frac{\sigma(T) a n^\eta}{k_B T}\right] \quad (4)$$

Here  $\rho_0(T)$  gives the temperature variation of the density due to single-particle excitations across the electron and hole Fermi surfaces, and the second term gives that corresponding to bubble fluctuations. Complete symmetry between droplet and bubble fluctuations has been assumed which gives a particularly simple expression for the density at the critical temperature

$$\rho_c = \frac{1}{2} \rho_0(T = T_c) \quad (5)$$

The shape of the phase diagram in the region  $T \geq \frac{1}{2}T_c$  is given by the sums in Eqs. (2) and (4) which correspond to fluctuations. As  $T$  approaches  $T_c$ ,  $\sigma(T)$  decreases and the fluctuations increase. Thus, crudely speaking, the shape of the phase diagram is controlled by  $\sigma(T)$ . In the droplet model, rather than employing an expression for the free energy as a function of the average uniform density, model averages are made over different configurations which consist of dense droplets and empty background (dense background and empty bubbles on the liquid side). Thus this approach has the merits that the free energy as a function of equilibrium density in the intermediate density regime is not required, and also critical fluctuations are included in a simple and intuitive way. In order to proceed further with quantitative calculation (or analysis of experiment) however, a further assumption must be made: that the bulk and surface-free energy of a droplet can be calculated as if it were in equilibrium rather than a part of a fluctuation configuration. This is obviously a good description when the lifetime of the fluctuation is long compared to the thermalization time of the droplet, which is expected to be the case for temperatures approaching  $T_c$ .

It is also worth pointing out that the simple picture of the gas phase used here does not account in an accurate way for the energetics of small, bound-state constituents (such as excitons, trions, etc.). There is some evidence<sup>22</sup> in unstrained Ge that their dissociation in the gas modifies the gas side of the condensation phase diagram for densities up to but not including the immediate vicinity of  $\rho_c$ . Such an effect is not included here, and for this reason also the present treatment is expected to give a good description of the phase diagram only for  $T$  near  $T_c$ .

### B. Microscopic calculations of the temperature-dependent surface tension for six model systems

In this section microscopic calculations of the temperature-dependent surface tension and resulting estimates of the critical temperatures and densities  $T_c$  and  $\rho_c$  are given for Ge and Si with varying strain along [111] and [100], respectively. The band

TABLE I. Input parameters for the calculations for six model systems. Ge[ $\nu_e; \nu_h$ ] indicates Ge with  $\nu_e$  and  $\nu_h$  occupied electron and hole bands. The masses give the transverse ( $\perp$ ) and longitudinal ( $\parallel$ ) masses of ellipsoidal electron and hole bands and heavy ( $H$ ) and light ( $L$ ) hole bands; masses are in units of the bare electron mass.  $R_0$  and  $a_0$  are effective Rydberg and Bohr radius, and  $D, E$  give bulk correlation energy [Eq. (7)].

	Ge[4;2]	Ge[1;2]	Ge[1;1]	Si[6;2]	Si[2;2]	Si[2;1]
$m_{e\perp}$	0.082	0.082	0.082	0.1905	0.1905	0.1905
$m_{e\parallel}$	1.58	1.58	1.58	0.9163	0.9163	0.9163
$m_{hH}$	0.347	0.347	$m_{h\perp}=0.130$	0.523	0.523	$m_{h\perp}=0.256$
$m_{hL}$	0.042	0.042	$m_{h\parallel}=0.040$	0.154	0.154	$m_{h\parallel}=0.200$
$2R_0$ (meV)	5.318	5.318	5.310	25.959	25.959	25.739
$a_0$ ( $10^{-6}$ cm)	1.763	1.763	1.766	0.487	0.487	0.491
$D$ ( $2R_0$ )	0.823	0.428	0.287	0.629	0.384	0.297
$E$	0.999	0.410	0.192	0.616	0.270	0.191

parameters for these systems are listed in Table I. The notation  $X[\nu_e; \nu_h]$  indicates system  $X$  ( $=$  Ge or Si) with  $\nu_e$  degenerate ellipsoidal electron conduction valleys and with a valence band composed of  $\nu_h$  (coupled) hole bands. A commonly used nomenclature is that Ge[4;2] and Si[6;2] are at "zero" strain, Ge[1;2] and Si[2;2] are at "intermediate" strain, and Ge[1;1] and Si[2;1] are at "large" strain. It may be noted that some recent experiments<sup>6,7</sup> have been carried out at a strain sufficient to remove both conduction- and valence-band degeneracies but which is not sufficiently large to correspond to the band structures in Table I; this arises because residual valence-band coupling gives an effectively nonpara-

bolic hole mass. This effect can be incorporated straightforwardly in the present calculations by modifying the kinetic energy of the holes.<sup>23</sup> Results for the systems in Table I will be obtained here first, and then in Sec. III A the effects of valence-band nonparabolicity for one particular experimental strain will be discussed.

The method used for calculating the temperature-dependent surface tension is essentially that given in Ref. 16 which is based on generalization of the approach used by Hohenberg and Kohn<sup>24</sup> for the inhomogeneous electron gas. The droplet free energy is written as a functional of the electron and hole densities  $\rho_e$  and  $\rho_h$  and is expanded in their gradients.

$$F[\rho_e, \rho_h] = \frac{e^2}{2\epsilon_0} \iint [\rho_h(\vec{r}) - \rho_e(\vec{r})][\rho_h(\vec{r}') - \rho_e(\vec{r}')]/|\vec{r} - \vec{r}'| d^3r d^3r' + \int g(\rho_e, \rho_h) d^3r + \int [g_e(\vec{r}) |\vec{\nabla} \rho_e|^2 + g_h(\vec{r}) |\vec{\nabla} \rho_h|^2 + g_{e,h}(\vec{r}) \vec{\nabla} \rho_e \cdot \vec{\nabla} \rho_h + \dots] d^3r \quad (6)$$

The bulk band structure is used for the energy versus wave-vector relation of electrons and holes. The carriers interact via a Coulomb potential screened by the static background dielectric constant  $\epsilon_0$ . The term involving  $g$  gives the local contribution to the free energy, and those involving  $g_e, g_h,$  and  $g_{e,h}$  give the leading gradient contributions; they are all in general temperature dependent.

For the local term in the free energy we use

$$g(\rho_e(\vec{r}), \rho_h(\vec{r})) = \frac{3}{10} (3\pi^2)^{2/3} \left\{ \frac{m_0 \rho_e^{5/2}}{m_{de}} \left[ 1 - \frac{5\pi^2}{12} \left( \frac{k_B T}{E_{F,e}} \right)^2 + \dots \right] + \frac{m_0 \rho_h^{5/3}}{m_{dh}} \left[ 1 - \frac{5\pi^2}{12} \left( \frac{k_B T}{E_{F,h}} \right)^2 + \dots \right] \right\} - \frac{3}{4} \left( \frac{3}{\pi} \right)^{1/3} \left[ \frac{\Phi(m_{e\perp}/m_{e\parallel})}{\nu_e^{1/3}} \rho_e^{4/3} + \Phi_h \rho_h^{4/3} \right] - D \left[ \frac{\rho_e^{4/3}}{E + \rho_e^{1/3}} + \frac{\rho_h^{4/3}}{E + \rho_h^{1/3}} \right], \quad (7)$$

where

$$m_{de} = \nu_e^{2/3} (m_{e\perp}^2 m_{e\parallel})^{1/3},$$

$$m_{dh} = \begin{cases} m_{hH} (1 + \gamma^{3/2})^{2/3} & \text{for "zero" and "intermediate" stress,} \\ (m_{h\parallel} m_{h\perp}^2)^{1/3} & \text{for "large" stress,} \end{cases}$$

and

$$\gamma = \frac{m_{hL}}{m_{hH}} .$$

The total effective optically averaged mass is

$$\frac{1}{m_0} = \begin{cases} \frac{1}{3} \left( \frac{1}{m_{e\parallel}} + \frac{2}{m_{e\perp}} \right) + \frac{1}{2} \left( \frac{1}{m_{hH}} + \frac{1}{m_{hL}} \right) & \text{for "zero" and "intermediate" stress ,} \\ \frac{1}{3} \left( \frac{1}{m_{e\parallel}} + \frac{2}{m_{e\perp}} \right) + \frac{1}{3} \left( \frac{1}{m_{h\parallel}} + \frac{2}{m_{h\perp}} \right) & \text{for "large" stress .} \end{cases}$$

The function  $\Phi_h$  is given by

$$\Phi_h = \begin{cases} \Psi(\gamma) & \text{for zero and intermediate stress ,} \\ \Phi(m_{h\perp}/m_{h\parallel}) & \text{for large stress .} \end{cases}$$

The functions  $\Phi$  and  $\Psi$  are given in Ref. 5. The Fermi energies are

$$E_{Fi}(\bar{r}) = [3\pi^2 n_i(\bar{r})]^{2/3} (m_0/2m_{di}), \quad i = e, h .$$

Atomic units are used throughout: The Bohr radius is  $a_0 = \epsilon_0 \hbar^2 / m_0 e^2$ , densities are in units of  $a_0^{-3}$ , and energy is in a.u. =  $2R_0 = e^2 / \epsilon_0 a_0$  where  $R_0$  is the "excitonic" Rydberg.

The first two terms in the local energy density Eq. (7) at  $T=0$  give the Hartree-Fock energy, which is calculated exactly.<sup>5</sup> The last term is the  $T=0$  correlation energy which is obtained by fitting calculations of the bulk correlation energy from Refs. 9, 10, and 25 (see Ref. 26) with a Wigner-like form. These calculations of the bulk correlation energy are the most detailed available and include in an approximate fashion both band anisotropy effects and multiple scattering effects. The resulting values<sup>28</sup> of  $D$  and  $E$  are given in Table I. The temperature-dependent terms in the bulk free energy Eq. (7) are the leading contributions in  $k_B T / E_{Fi}$  from the noninteracting kinetic energy only. The temperature dependence of the exchange-correlation energy has been neglected; this is expected to be a good approximation because Rice<sup>29</sup> has shown that (at least for Ge[4;2]) the combined effect of exchange and correlation on the single-particle properties is to lower the electron and hole bands rigidly.

The leading contributions to the coefficients of the gradient terms  $g_e, g_h$  in the high-density limit are obtained from the kinetic energy functional only, and they are<sup>30</sup>

$$g_i = g_i(0) \left[ 1 + \left( \frac{1}{3} \pi^2 \right) (k_B T / E_{Fi})^2 + \dots \right] , \quad (8)$$

where

$$g_e(0) = \frac{m_0}{m_{e0}} \left( \frac{1}{72\rho_e} \right) , \quad (9a)$$

$$g_h(0) = \frac{(1 + \gamma^{1/2})(m_0/m_{hH})}{1 + \gamma^{3/2}} \left( \frac{7}{72\rho_h} \right) - \frac{\gamma^{1/2}(m_0/m_{hH})}{(1 + \gamma^{3/2})(1 + \gamma^{1/2})} \left( \frac{1}{3\rho_h} \right) , \quad (9b)$$

and

$$m_{e0}^{-1} = \frac{1}{3} \left( \frac{1}{m_{e\parallel}} + \frac{2}{m_{e\perp}} \right) .$$

Retaining the leading coefficients in the kinetic energy functional only should be a good approximation for EHD systems because of their high effective density,  $r_s \leq 1.5$  ( $r_s$  is the interparticle spacing divided by  $a_0$ ). Rose and Shore<sup>31</sup> have shown explicitly (for Ge[4;2] at  $T=0$ ) that a good approximation to the exact kinetic energy is obtained by retaining its leading gradient term only as done here. In addition, it has been shown that approximating the exchange and correlation energies by a local term only, as done here, gives good agreement with Hartree-Fock calculations for atoms<sup>32</sup> and that this approximation satisfies an important sum rule in the case of surface calculations.<sup>33</sup> In Eq. (8) as in Eq. (7) the leading term in  $k_B T / E_{Fi}$  has been retained. Band-structure effects have been included fully except that the hole bands have been taken to be isotropic.

We shall be concerned with temperatures up to the critical temperature for each system, and it is found that for such temperatures  $k_B T / E_{Fi} \ll 1$  where  $E_{Fi}$  is the Fermi energy evaluated at the equilibrium bulk density. This is the basis for retaining only the leading terms in  $k_B T / E_{Fi}$  in the free-energy functional, Eqs. (7) and (8). The equilibrium EHL density  $\rho_0(T)$  and its surface tension  $\sigma(T)$  therefore will be

expanded for small  $T$  in a similar fashion

$$\rho_0(T) \cong \rho_0(0)(1 - \delta_\rho T^2) , \quad (10a)$$

$$\sigma(T) \cong \sigma(0)(1 - \delta_\sigma T^2) . \quad (10b)$$

The density  $\rho_0(T)$  is obtained by minimizing the bulk free energy per electron-hole pair, Eq. (7). This gives the values for  $\rho_0(0)$  and  $\delta_\rho$  quoted in Table II.<sup>34</sup>

In order to obtain the surface tension the electron and hole densities ( $i = e, h$ ) in the surface region are parameterized by the planar forms

$$\rho_i = \begin{cases} \frac{1}{2} \rho_0(T) \exp(-\beta_i x), & x > 0 , \\ \rho_0(T) - \frac{1}{2} \rho_0(T) \exp(\beta_i x), & x < 0 , \end{cases} \quad (11)$$

where  $x$  is the distance perpendicular to the surface. For a fixed  $T$  the quantity  $\sigma(\beta_i, T)$

$$\sigma(\beta_i, T) = \frac{1}{A} (F[\rho_e, \rho_h] - F[\rho_0, \rho_0])$$

is formed as a function of the parameters  $\beta_i$  by (numerical) integration of Eq. (11). Then the surface tension  $\sigma(T)$  (and  $\beta_i$ ) are obtained by minimizing  $\sigma(\beta_i, T)$  with respect to the variational parameters  $\beta_i$ ,

$$\frac{d\sigma(\beta_i, T)}{d\beta_i} = 0, \quad i = 1, 2 . \quad (12)$$

$\sigma(T)$  is obtained as an expansion in small  $T$  as in Eq. (10b), and the results are given in Table II.

Within the droplet fluctuation model the critical temperature for EHD condensation is given by the temperature at which the droplet surface tension goes to zero, Eq. (3). From Eq. (10b) this gives

$$T_c \cong (\delta_\sigma)^{-1/2} . \quad (13)$$

The values of  $T_c$  obtained in this way from the calculations of  $\sigma(T)$  are given in Table II for the six model systems.<sup>36</sup> The corresponding values of the

critical density  $\rho_c$  obtained from Eq. (5) are also given.

We have also considered in detail the effects which several approximations in our calculation of the surface tension have on  $T_c$  [and on  $\sigma(0)$ ]. The most important of these approximations is found to be the treatment of the contribution to the surface tension from the low-density "tail" region of electron and hole distributions. The free-energy functional used here is appropriate for a high-density electron-hole system and does not represent properly the low-density tail region. The contribution of the local term, Eq. (7), to  $\sigma(T)$  from the tail region is negligible for large  $x$  and can be ignored; we have simply used expression (7) for all  $x$ . The contribution of the gradient term, Eqs. (6) and (8), for low densities such that  $E_{Fi}(\rho_i(x)) \leq k_B T$  however becomes artificially large. On the grounds that the low-density region should make a small contribution to  $\sigma(T)$ , we have made a physically plausible but somewhat arbitrary effective "cutoff" in the integration over  $x$  by evaluating  $E_{Fi}(\rho_i(x) = \bar{\rho})$  in Eq. (8) where  $\bar{\rho} = 0.4\rho_0(0)$ <sup>37</sup>; this gives the values for  $T_c$  in Table II. By varying  $\bar{\rho}$  between  $0.3\rho_0(0) \leq \bar{\rho} \leq 0.7\rho_0(0)$  the resulting values of  $T_c$  vary by  $\leq (\frac{+8}{-5})\%$ .<sup>38</sup> Other checks on the approximations used in the present calculation include using the eight term polynomial fit (of Ref. 35) for the correlation energy which decreases  $T_c$  by  $\leq 7\%$  and decreases  $\sigma(0)$  by a similar amount and, secondly, including a term corresponding to the leading contribution of the exchange and correlation energy to the gradient term in Eq. (6), which decreases  $T_c$  by  $\sim 4\%$ . We feel that a reasonable estimate of the total uncertainty in  $T_c$  from the approximations involved in the present calculation is  $\sim \pm 8\%$ .

The values obtained here for  $\sigma(0)$ , the zero-temperature surface energy, are in agreement with those reported previously by the present authors<sup>14, 16, 39, 40</sup> for Ge[4;2], Si[6;2], and Ge[1;1] and

TABLE II. Values of the bulk density and surface tension [Eq. (10)], and of the critical temperature and density  $T_c$  and  $\rho_c$  obtained from calculations in text.  $\sigma(0)a_0/k_B T_c$  characterizes the shape of the corresponding phase diagram.

	Ge[4;2]	Ge[1;2]	Ge[1;1]	Si[6;2]	Si[2;2]	Si[2;1]
$\rho_0(0)$ ( $10^{17}$ cm <sup>-3</sup> )	2.258	0.717	0.111	32.51	13.80	4.494
$\delta_\rho$ ( $10^{-3}$ K <sup>-2</sup> )	9.2444	18.04	49.90	0.7427	1.012	1.827
$\sigma(0)$ ( $10^{-4}$ erg/cm <sup>2</sup> )	1.84	0.452	0.0679	32.0	11.6	3.53
$\delta_\sigma$ ( $10^{-2}$ K <sup>-2</sup> )	2.21	4.18	11.8	0.181	0.283	0.495
$T_c$ (K)	6.73	4.89	2.91	23.5	18.8	14.2
$\rho_c$ ( $10^{17}$ cm <sup>-3</sup> )	0.656	0.204	0.0320	9.59	4.43	1.42
$\sigma(0)a_0/k_B T_c$	2.56	1.87	1.63	2.17	1.75	1.48

are in reasonably good agreement with the calculations reported by other authors.<sup>31,35,41-44</sup> In particular for the case of Ge[4;2], the present results are in very good agreement with the recent detailed calculations of Rose and Shore<sup>31</sup> in the case in which these authors use essentially the same ( $T=0$ ) energy functional used here. There is at present some uncertainty as to whether it is appropriate to include the leading effects of exchange and correlation in the gradient term in energy functional, Eq. (6), and we have not included them above.<sup>32,33</sup> We find, in agreement with other authors,<sup>31,43,44</sup> that the effect of such terms is to increase  $\sigma(0)$ . In the case of Ge[1;1], for example, if we include the leading contributions from the exchange and correlation in the high-density limit<sup>44</sup> to the gradient term ( $g_e^{xc} + g_h^{xc}$ ) = 5.083  $\times 10^{-3} [\frac{1}{2}(\rho_e + \rho_h)]^{-4/3}$  a.u.,  $\sigma(0) = 0.112 \times 10^{-4}$  erg/cm<sup>2</sup> which is somewhat larger than that given in Table II (and first reported by us for this system<sup>39</sup>) and is in fairly good agreement with recent calculations by others.<sup>31,35,41,43,44</sup> Finally it might be noted that the apparently large change with stress in the numerical value of  $\sigma(0)$  between the several model systems studied here is consistent with the crude rule that on dimensional grounds  $\sigma(0)$  should scale roughly with  $\epsilon_g \rho_0(0)^{2/3}$  where  $\epsilon_g$  is the EHL ground-state energy at density  $\rho_0(0)$ .

### C. Phase diagrams for six model systems

Equations (2) and (4) give the phase diagram in terms of  $\sigma(T)$  and  $\rho_0(T)$  which are properties of the low-temperature EHL. In Figs. 2 and 3 we give the phase diagrams obtained by using the results of the microscopic calculations from Sec. II B for  $\sigma(T)$  and  $\rho_0(T)$  for Ge and Si, respectively, with varying strain. In each of these systems for temperatures less than the critical temperature,  $\rho_0(T)$  and  $\sigma(T)$  can be expanded for small  $T$  as in Eqs. (10). From simple geometry

$$\begin{aligned} a &= 4\pi [3/[4\pi\rho_0(T)]]^{2/3} \\ &= 4\pi [3/[4\pi\rho_0(0)]]^{2/3} [1 + \frac{2}{3}\delta_\rho T^2] \end{aligned} \quad (14)$$

and  $\eta = \frac{2}{3}$ ; also  $\tau = 2.2$ .<sup>45</sup> Then  $q_0 = \rho_c/\zeta(\tau-1)$  where  $\zeta(\cdot)$  is the Riemann  $\zeta$  function.

The simple droplet fluctuation model given in Sec. II A for EHD condensation and for the phase curve is based on the standard ideas of equilibrium statistical mechanics and does not take into account effects resulting from the finite lifetime  $\tau_0$  of the electron and hole which characterizes EHD. Detailed calculations<sup>46,47</sup> based on a model which treats evaporation, collection, and recombination processes at the droplet have shown that there are differences between the condensation phase curve (on the low- $T$  gas side) for

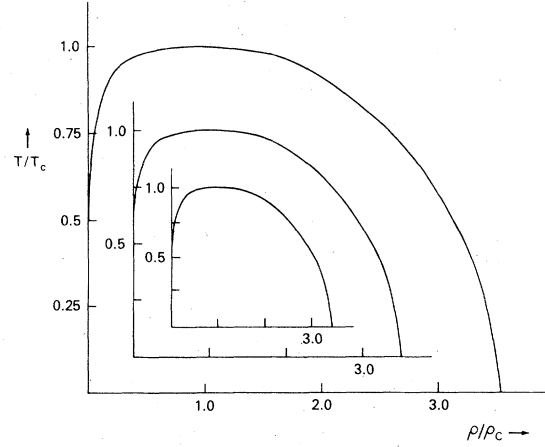


FIG. 2. Phase diagrams obtained from calculations in text for Ge with zero, intermediate, and large uniaxial strain.

$\tau_0$  infinite and for the finite  $\tau_0$  which corresponds to real EHD systems. Physically the reason that the effects of finite  $\tau_0$  become non-negligible only at low  $T$  is that for such temperatures the rates for the evaporation and collection processes slow down to the time scale of  $\tau_0$ . For Ge[4;2] and Si[6;2] these deviations are found to occur only for  $T \leq 2$  K and  $T \leq 8$  K, respectively, and in the region  $T \geq \frac{1}{2}T_c$  of particular interest here there is no appreciable difference for finite and infinite  $\tau_0$ . Because the critical temperatures decrease substantially with strain however, it becomes important to determine for what temperatures the effects of finite  $\tau_0$  become appreciable in strained systems, but detailed calculations of the effects of finite  $\tau_0$  for these systems are not yet available.

A rough estimate of these temperatures can be obtained by noting that the difference between the

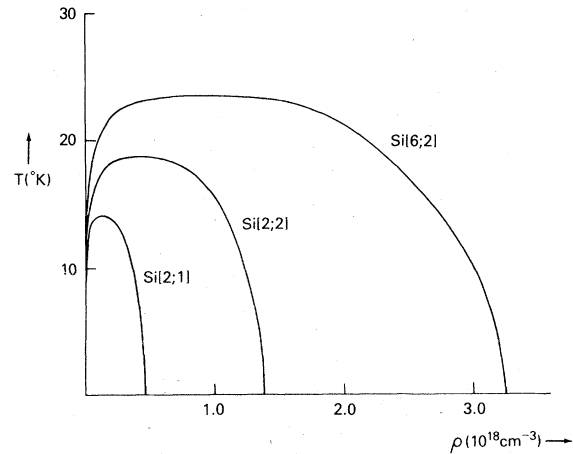


FIG. 3. Phase diagrams obtained from calculations in text for Si with zero, intermediate, and large uniaxial strain.

phase curve (on the gas side) for finite  $\tau_0$  and infinite  $\tau_0$  depends on  $(\mu_G - \mu_l)/k_B T$  where  $\mu_G$  and  $\mu_l$  are the (true) chemical potentials for the gas and the liquid for infinite  $\tau_0$ . A convenient estimate<sup>48</sup> of the temperature below which the effects of finite  $\tau_0$  become appreciable in strained systems can therefore be made by determining the temperature for which this ratio in the strained system equals that for the corresponding unstrained system evaluated at the temperature for which finite  $\tau_0$  effects are known from available detailed calculations to become appreciable in the latter systems. A lower bound for  $(\mu_G - \mu_l)/k_B T$  is given by Silver<sup>46,49</sup>

$$\frac{\mu_G - \mu_l}{k_B T} \geq \ln \left[ 1 + \left( \frac{2\sigma(0)}{3AT^3\tau_0 k_B} \right)^{1/2} \exp \left( \frac{\phi}{k_B T} \right) \right], \quad (15)$$

where  $A$  is the coefficient of the Richardson-Dushman expression for exciton evaporation from the drop, and  $\phi$  is the condensation energy (the difference between the EHD ground-state energy and the exciton energy). By using the above procedure<sup>50</sup> we have determined for example that finite  $\tau_0$  is expected to have an appreciable effect on the phase diagram for Ge[1;1] only for  $T \lesssim \frac{1}{2}$  K and for Si[2;1] only for  $T \lesssim 2$  K. Physically the reason why these temperatures decrease for increasing stress is that the effects of finite  $\tau_0$  depend on temperature mainly through  $\exp(\phi/k_B T)$  (which arises from the evaporation term), and  $\phi$  decreases with increasing strain. In fact, we find for all of the six systems studied the effects of finite  $\tau_0$  are negligible for  $T \gtrsim \frac{1}{2} T_c$ , the region of interest here.

### III. COMPARISON WITH EXPERIMENT, WITH OTHER CALCULATIONS, AND DISCUSSION

#### A. Comparison with experiment

Complete phase diagrams have been measured only for Ge[4;2]<sup>12,22</sup> and for Si[6;2]<sup>55-57</sup>; such data are shown in Figs. 4(a) and 4(b). For Ge[4;2] the most recent measurements of  $T_c$  and  $\rho_c$  by Thomas *et al.*<sup>22</sup> give  $T_c = 6.7 \pm 0.2$  K and  $\rho_c = (6 \pm 1) \times 10^{16}$  cm<sup>-3</sup> and by Minescalco *et al.*<sup>58</sup> give  $T_c = 7.0 \pm 0.1$  K and  $\rho_c = (8.9 \pm 0.5) \times 10^{16}$  cm<sup>-3</sup>; earlier measurements by Thomas *et al.*<sup>12</sup> gave  $T_c = 6.5 \pm 0.1$  K and  $\rho_c = (8 \pm 2) \times 10^{16}$  cm<sup>-3</sup>. For Si the most recent measurements of the critical point by Forchel and Schmid<sup>56</sup> give  $T_c = 22.5 \pm 1.0$  K and  $P_c = (1.34 \pm 0.03) \times 10^{18}$  cm<sup>-3</sup> and measurements by Shah *et al.*<sup>55</sup> give  $T_c = 27 \pm 1$  K and  $\rho_c = 1.1 \times 10^{18}$  cm<sup>-3</sup>. Clearly the results of the microscopic calculations presented here (Table II) are in quite good agreement with recent experimental values for  $T_c$  and in reasonable agreement for  $\rho_c$  (for which experimental values are probably somewhat less reliable).

Somewhat less detailed measurements of the phase diagram for uniaxially stressed Ge have been reported recently by Feldman *et al.*<sup>7</sup> At the stress employed in this experiment the electron- and hole-band degeneracies are lifted, but residual valence-band coupling gives a valence band which is nonparabolic, with a hole mass which effectively depends on the energy.<sup>7,23</sup> The band structure of this system therefore does not quite correspond to the model Ge[1;1] treated above. Also a detailed calculation of the correlation energy has not yet been carried out for the band structure corresponding to the experimental stress. In order to make a comparison with these experimental results, we have made an estimate of  $T_c$  and  $\rho_c$  based on the method of Sec. II B as follows: We first note that the total of the exchange and correlation energies when expressed in the appropriate atomic units as a function density also in atomic units is very nearly independent of system.<sup>59-61</sup> Therefore the exchange and correlation energy of Ge[1;1] is used in the bulk term Eq. (7). Then the hole density of states mass is adjusted so as to give the ground-state equilibrium density  $\rho_0(0) = 2.7 \times 10^{16}$  cm<sup>-3</sup> observed in the experiment.<sup>7</sup> The adjusted hole density of states mass is used in  $E_{FH}$ , and the gradient coefficients for Ge[1;1] are retained. The surface tension and equilibrium density are calculated as usual and are found to be

$$\sigma(T) = 0.150[1 - (0.0825 \text{ K}^{-2}) T^2] \times 10^{-4} \text{ erg/cm}^2$$

and

$$\rho_0(T) = 2.7[1 - (0.03869 \text{ K}^{-2}) T^2] \times 10^{16} \text{ cm}^{-3}.$$

From these results we obtain  $T_c = 3.53$  K and  $\rho_c = 0.699 \times 10^{16}$  cm<sup>-3</sup>. These values are in good agreement with the experimental results which are  $T_c = 3.5 \pm 0.5$  K and  $\rho_c = (0.77 \pm 0.2) \times 10^{16}$  cm<sup>-3</sup>. The complete phase diagram is readily calculated as in Sec. II C and is found to be in good agreement with the available data.<sup>7</sup>

In comparing the phase diagrams with experiment it should be pointed out that there is at present considerable uncertainty concerning the gas side of the phase diagram. Recently, based on an analysis of recombination line shapes, Thomas *et al.*<sup>22</sup> have concluded in the case of unstrained Ge that the gas side of the phase diagram for densities up to but not including the immediate vicinity of  $\rho_c$  is modified as a result of progressive dissociation with increasing density of the constituents (excitons, trions, etc.) of the gas. This effect is not yet entirely clarified experimentally or theoretically.

The phase diagrams obtained in Sec. II C on the basis of microscopic calculations of  $\rho_0(T)$  and  $\sigma(T)$  are in generally good agreement with experiment for Ge[4;2] and Si[6;2] as noted above. The most discerning test of the droplet fluctuation model, howev-

er, is given by using the experimentally determined  $\rho_0(T)$  and  $\sigma(T)$  to fit the data for the phase diagram near  $T_c$ . This fitting procedure in addition allows an estimate of the surface-energy parameter  $\sigma(0)$  to be extracted from measurements of the phase diagram. Such fits have been made for the data for Ge[4;2]<sup>14</sup> and Si[6;2]<sup>17</sup> and the results are shown in Figs. 4(a)<sup>62</sup> and 4(b).  $\rho_0(T)$  was obtained from the low- $T$  liquid side of the phase diagram and is shown by  $\rho_0$  in the figures;  $\delta_\sigma$  is given by  $T_c^{-2}$  [see Eq. (13)] where  $T_c$  is obtained from experiment.<sup>63</sup> Finally  $\sigma(0)$  is chosen in order to give the best overall fit to the data in each case. The values of the droplet fluctuation surface-energy parameter  $\sigma(0)$  obtained in this way are  $\sigma(0) = 1.0 \times 10^{-4}$  erg/cm<sup>2</sup> for Ge[4;2] and  $\sigma(0) = 32 \times 10^{-4}$  erg/cm<sup>2</sup> for Si[6;2]. Clearly the present model accounts well for the detailed features of the phase diagrams.

The interpretation of the surface-energy parameter  $\sigma(0)$  for the droplet fluctuations appearing in Eqs. (2) and (4) as the surface-energy appropriate to large equilibrium drops must be taken with some caution. Except for  $T$  quite near  $T_c$  the sums in Eqs. (2) and (4) are dominated by relatively small droplet fluctuations. For example, in the case of Ge[4;2] shown in Fig. 4(a) ( $T_c = 6.5$  K) at  $T = 5.5$  and 6.4 K,  $n \geq 10$  and  $n \geq 30$  contribute  $\leq 10\%$  of the sums. In principle, more reliable values of the surface tension could be obtained by fitting the phase diagram within a few tenths of a degree of  $T_c$ , but sufficiently detailed experimental data is not available in this region. For small droplet fluctuations the separation of the free energy into bulk and surface terms is somewhat arbitrary, and the surface-energy parameter appropriate for the relatively small droplet fluctuations on the phase curve may differ somewhat from that for a large droplet. This difference has two closely related implications for the present treatment of EHD phase diagrams. First, there is some uncertainty in interpreting the value for  $\sigma(0)$  obtained by fitting experimental data for the phase diagram as done in Figs. 4(a) and 4(b) as the surface energy of large drops, and second there is a corresponding uncertainty in using values of the surface energy calculated microscopically for a large planar surface as in Sec. II B as the surface energy appropriate for the small droplet fluctuations in constructing the phase diagrams.

Although the relationship between the surface energy for the droplet fluctuations on the phase diagram and that for larger droplets is not yet known in detail, an estimate can be obtained by examining the case of Ge[4;2] for which experimental estimates based on other methods are available. Analysis of nucleation data<sup>47,64-66</sup> and of acoustic absorption<sup>67</sup> has given estimates of the surface energy for large droplets in the range  $(2.1-4.2) \times 10^{-4}$  erg/cm<sup>2</sup> which, although there remains considerable variation in the values, nevertheless give values which are consistent-

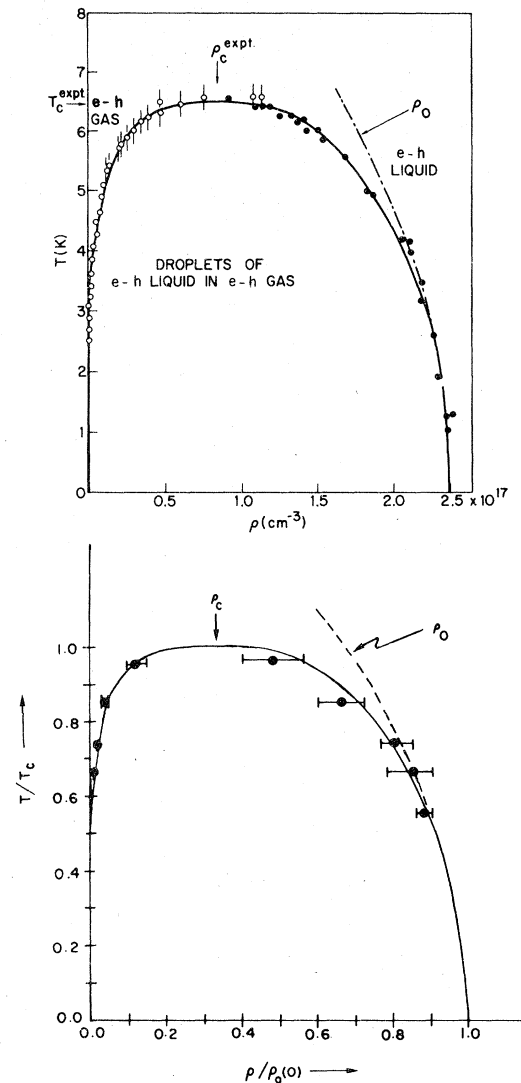


FIG. 4. Comparison between droplet fluctuation model (solid curves) and measurements of electron-hole droplet phase diagrams: (a) for Ge (data from Ref. 12; see Ref. 62), and (b) for Si (data from Ref. 55).

ly somewhat larger than the value  $1 \times 10^{-4}$  erg/cm<sup>2</sup> obtained by fitting the phase curve [Fig. 4(a)]. By noting that at a given value of  $T/T_c$  similar percentages of the sums for the phase curve for all systems studied are given by fluctuations of a similar size, we are led to suggest that the relationship between the surface-energy parameter for droplet fluctuations on the phase curve and that for large droplets is roughly the same in all systems. Specifically, the surface energy for large droplets appears to be roughly three times that obtained by fitting the phase curve. Thus,

for example, on the basis of the fitting of the phase diagram for Si[6;2] above [Fig. 4(b)] we estimate that the surface energy for large drops in Si is  $\approx 100 \times 10^{-4}$  erg/cm<sup>2</sup>. This value is consistent with a recent estimate made for Si[6;2] on the basis of nucleation data.<sup>54</sup>

#### B. Comparison with results of the uniform plasma approach

The values of the critical temperatures and densities for these six systems calculated above from the droplet fluctuation model are now compared to the corresponding values calculated from the "uniform plasma approach"<sup>68</sup> to the EHD critical region. The basic idea behind the uniform plasma approach to the critical point is understood by noting that in principle for  $T < T_c$  the sides of the coexistence curve can be obtained by using a Maxwell construction involving the chemical potential  $\mu$  as a function of density  $\rho$  and that the critical point is given by an inflection point in  $\mu$  vs  $\rho$ . Combescot<sup>68</sup> has pointed out that despite the fact that an expression for the free energy like that in Eq. (7) is too crude for an adequate description of the gas phase along the phase boundary and hence cannot be used to determine directly the phase diagram, the critical point itself occurs at a fairly high density and the free-energy expression (7) and the chemical potential derived from it provides a reasonable description there. Thus the inflection point in the corresponding chemical potential can be used to determine  $T_c$  and  $\rho_c$ .

We have recently made new calculations of the critical point based on this approach using a chemical potential formed from a free energy which is essentially that in Eq. (7) except that the numerical values of the correlation energies from Refs. 9, 10, and 25 were used directly at the densities for which they were tabulated and a Wigner-like form was used for lower densities. Analogous calculations made using an eight-term polynomial fit to the correlation energies gave only modest ( $\sim 5\%$ ) changes for  $T_c$ . The dependence of the resulting critical points on details of the correlation energy was tested by studying its changes resulting from arbitrary changes in the density derivatives of the correlation energy, and the criti-

cal point was found not to be overly sensitive to details of the correlation energy. The results are shown in Table III.

Points to be noted from these results include: (i) An error in previous calculations<sup>69</sup> was corrected. (ii) These results for the critical point, especially for  $T_c$  are in rather good agreement with those obtained by other authors<sup>12,68,70</sup> who used the uniform plasma approach but used somewhat different correlation energies. This agreement as well as the results of the direct tests of the sensitivity of the critical point to details of the correlation energy indicate that this approach gives consistent estimates of the critical point which are not strongly dependent on an imperfect knowledge of the correlation energy. (iii) The resulting values of  $T_c$  are larger than the most recent experimental results<sup>22,56,58</sup> and also than the results of the present droplet fluctuation model calculations.

The droplet fluctuation model and the uniform plasma approach employ two rather different treatments of the EHD system at its critical point. In the uniform plasma approach the chemical potential is calculated neglecting statistical density fluctuations, and the critical point is located from an inflection point in the chemical potential. In the present droplet fluctuation model, on the other hand, statistical density fluctuations are included in an approximate way, and  $T_c$  is obtained from the temperature dependence of the surface tension. The nature of the two approximations is different, and the accuracy of each is difficult to estimate; thus it does not appear that one can distinguish *a priori* which is the better method with which to estimate the critical point. As seen from Tables II and III, the values of  $T_c$  from the uniform plasma approach are in reasonable good agreement with those from the droplet fluctuation model but are consistently somewhat higher than the latter results; importantly they show the same trend with strain. The fact that the uniform plasma approach gives values of  $T_c$  consistently higher than those from the droplet fluctuation model is consistent with the fact that in the former approach critical fluctuations are neglected. In all such mean-field-like approaches which neglect fluctuations, the critical temperature is overestimated.<sup>71</sup> The droplet fluctuation model, on the other hand, includes fluctuations albeit

TABLE III. Values of the critical parameters calculated on the basis of the uniform plasma model approach to the critical point.

	Ge[4;2]	Ge[1;2]	Ge[1;1]	Si[6;2]	Si[2;2]	Si[2;1]
$T_c$ (K)	7.91	6.09	3.76	29.1	26.4	17.6
$\rho_c$ ( $10^{17}$ cm <sup>-3</sup> )	0.436	0.117	0.0247	4.22	2.71	0.779

in an approximate way.

Finally it should also be noted that the droplet fluctuation model gives the critical point as a part of a unified treatment of the phase diagram near  $T_c$  whereas the uniform plasma approach gives only the quantities  $T_c$  and  $\rho_c$ .

### C. Discussion

Finally we point out that the present droplet fluctuation model provides a useful parameter with which to characterize quantitatively the "shape" of the EHD phase diagram. As the number of systems in which EHD condensation is studied has increased in recent years to include stressed Ge and Si and also a variety of compound semiconductors, interest has grown in the systematics of this phenomenon, e.g., in the extent to which the features of the condensation are common to all systems or vary from system to system. One suggestion along these lines is that EHD phase diagrams have a universal shape which is in fact the same as that for a classical gas condensation.<sup>1</sup> From Eqs. (2), (10b), and (13), it is seen that each term in the sum for  $\rho_{G, \text{coex}}$  is a power of  $\exp\{-[\sigma(0)a(T)/T_c][1 - (T/T_c)^2]T_c/T\}$ , and similarly for  $\rho_{L, \text{coex}}$ . Thus in the region  $T \gtrsim \frac{1}{2}T_c$  the shape of the phase diagram when expressed in densities scaled by  $\rho_c$  and temperatures by  $T_c$  (i.e.,  $\rho/\rho_c$  vs  $T/T_c$ ) is characterized by the dimensionless quantity  $\sigma(0)a_0/k_B T_c \propto \sigma(0)/\rho_0(0)^{2/3}k_B T_c$  where  $a_0 = 4\pi[3/14\pi\rho_0(0)]^{2/3}$  from Eq. (14). As discussed in detail in Sec. IIB the quantities  $\sigma(0)$  and  $T_c$  are each sensitive (in different ways) to details of the EHL energetics, which itself is determined by the semiconductor band structure. Thus we expect *a priori* that the shape of the phase diagram will vary accordingly from system to system.<sup>72</sup> Values of the parameter  $\sigma(0)a_0/k_B T$  obtained from the microscopic calculations of  $\sigma(0)$  and  $T_c$  given above are listed in Table II for the six systems studied here. The shape of the corresponding phase diagrams is seen to have a systematic variation with strain in both Ge and Si. The decreasing value of the shape parameter with strain corresponds to a phase diagram which is less "flat" on the top. Because the values of  $\sigma(0)$  and  $T_c$  for the six systems were obtained by the same theoretical approach, we believe that this systematic variation with stress is real and that it reflects the underlying change in the energetics. Indeed, in very recent work in which we develop several "scaling relations" for EHD condensation we<sup>60</sup> have shown that this shape parameter for the phase diagram scales like

$\sigma(0)a_0/k_B T_c \propto (C/A)^{1/2}$  where  $C$  is the coefficient of  $|\nabla \rho|^2/\rho$  in the gradient term in the free energy ( $\rho_e = \rho_h = \rho$ ), Eqs. (6), (8), and (9), and  $A$  is the coefficient of  $\rho^{5/3}$  in the bulk term Eq. (7). We have shown that within approximations similar to those employed here the changes in the shape parameter with strain obtained in the present calculations can be accounted for quantitatively by the corresponding changes in  $(C/A)^{1/2}$ . Thus this scaling argument and the explicit calculations presented here substantiate the dependence of the shape of the phase diagram on the underlying droplet energetics (band structure).

### IV. CONCLUDING REMARKS

We have provided a model of electron-hole droplet condensation and of the corresponding phase diagram, which reduces the description of the entire phase diagram to the properties of the low-temperature electron-hole liquid. Detailed calculations of the surface tension for six model systems involving Ge and Si with varying uniaxial stress have been presented, and the corresponding phase diagrams have been constructed, thus providing a detailed picture of EHD condensation in a set of systems with systematically but widely varying energetics. Results for their critical points have been compared to the results of new calculations of the corresponding quantities based on the uniform plasma model. As the ground-state energetics of EHD in other systems are understood in better microscopic detail, this model will enable the construction of the corresponding phase diagrams, or conversely as the phase diagrams are measured in greater detail the model provides a method to extract an estimate of the droplet surface tension. Finally the droplet fluctuation model provides a convenient parameter with which to characterize quantitatively the shape of phase diagrams, and systematic changes in the shape of the phase diagram corresponding to systematic changes in the underlying energetics have been obtained.

### ACKNOWLEDGMENTS

One of us (M.C.L.) would like to thank R. K. Kalia for helpful advice. Two of us (M.C.L. and S.C.Y.) were supported in part by the NSF, Contract No. EMR73-07569, and by the Materials Sciences Program, Brown University.

- <sup>1</sup>For a review of the experimental literature see J. C. Hensel, T. G. Phillips, and G. A. Thomas, *Solid State Physics* 32, edited by F. Seitz, D. Turnbull, and H. Ehrenreich (Academic, New York, 1977), p. 88, and references therein.
- <sup>2</sup>For a review of the theoretical literature see T. M. Rice, *Solid State Physics* 32, edited by F. Seitz, D. Turnbull, H. Ehrenreich (Academic, New York, 1977), p. 1, and references therein.
- <sup>3</sup>Ref. 1, p. 242.
- <sup>4</sup>C. Benoit à la Guillaume, M. Voos, and F. Salvan, *Phys. Rev. B* 5, 3079 (1972); T. Ohyama, T. Sanada, and E. Otsuka, *Phys. Rev. Lett.* 33, 647 (1974); Ya. E. Pokrovsky and K. I. Svistunova, *Zh. Eksp. Teor. Fiz.* 68, 2323 (1975) [*Sov. Phys. JETP* 41, 1161 (1976)]; V. S. Bagaev, T. I. Galkina, and O. V. Gogolin, *Proceedings of the Tenth International Conference on Physics of Semiconductors, Cambridge, Massachusetts, 1970*, edited by S. P. Keller, J. C. Hensel, and F. Stern (U.S. AEC, Springfield, Va., 1970), p. 500; B. M. Ashkinadze, I. P. Kretsu, A. A. Patrin, and I. D. Yaroshetskii, *Phys. Status Solidi B* 46, 495 (1971); and references in these papers.
- <sup>5</sup>W. F. Brinkman and T. M. Rice, *Phys. Rev. B* 7, 1508 (1973); M. Combescot and P. Nozières, *J. Phys. C* 5, 2369 (1972).
- <sup>6</sup>H.-h Chou, G. K. Wong, and B. J. Feldman, *Phys. Rev. Lett.* 39, 959 (1977).
- <sup>7</sup>B. J. Feldman, H.-h Chou, and G. K. Wong, *Solid State Commun.* 24, 521 (1977); 26, 209 (1978).
- <sup>8</sup>G. A. Thomas and Ya. E. Pokrovskii, *Phys. Rev.* 12, 864 (1978).
- <sup>9</sup>P. Vashishta, Shashikala G. Das, and K. S. Singwi, *Phys. Rev. Lett.* 33, 911 (1974); P. Vashishta, P. Bhattacharyya, and K. S. Singwi, *Phys. Rev. B* 10, 5108 (1974).
- <sup>10</sup>P. Vashishta, S. G. Das, and K. S. Singwi, *Phys. Rev. Lett.* 33, 911 (1974).
- <sup>11</sup>G. A. Thomas, T. G. Phillips, T. M. Rice, and J. C. Hensel, *Phys. Rev. Lett.* 31, 386 (1973).
- <sup>12</sup>G. A. Thomas, T. M. Rice, and J. C. Hensel, *Phys. Rev. Lett.* 33, 219 (1974).
- <sup>13</sup>M. Droz and M. Combescot, *Phys. Lett. A* 51, 473 (1975).
- <sup>14</sup>T. L. Reinecke and S. C. Ying, *Phys. Rev. Lett.* 35, 311 (1975); 35, 547(E) (1975).
- <sup>15</sup>G. Mahler, *Phys. Rev. B* 11, 4050 (1975); G. Mahler and Joseph L. Birman, *Phys. Rev. B* 16, 1552 (1977).
- <sup>16</sup>T. L. Reinecke and S. C. Ying, *Phys. Rev. B* 13, 1850 (1976).
- <sup>17</sup>T. L. Reinecke, *Phys. Rev. B* 18, 2947 (1978).
- <sup>18</sup>J. Frenkel, *Kinetic Theory of Liquids* (Oxford University, Oxford, England, 1946), Chap. VII; W. Band, *J. Chem. Phys.* 7, 324 (1939); 7, 924 (1939); A. Bijl, Doctoral dissertation (Leiden, 1938) (unpublished).
- <sup>19</sup>M. E. Fisher, *Physics (N.Y.)* 3, 255 (1967); C. S. Kiang, *Phys. Rev. Lett.* 24, 47 (1970).
- <sup>20</sup>Only neutral fluctuations (with equal numbers of electrons and holes) are included here. Explicit calculations indicate that charged fluctuations make a relatively small contribution to the sums over fluctuations on the phase diagram because of their electrostatic self-energy (for Ge, for example, less than 12% of the sum for temperatures to within 0.1 K of  $T_c$ ).
- <sup>21</sup>Term  $\tau \ln n$  in the free energy arises from the entropy restriction that the droplet surface must close on itself.
- <sup>22</sup>G. A. Thomas, J. B. Mock, and M. Capizzi, *Phys. Rev. B* 18, 4250 (1978).
- <sup>23</sup>L. Liu, *Solid State Commun.* 25, 805 (1978); L. Liu and Lu Sun Liu, *Solid State Commun.* 27, 801 (1978).
- <sup>24</sup>P. Hohenberg and W. Kohn, *Phys. Rev.* 136, B864 (1964).
- <sup>25</sup>R. K. Kalia, Ph.D. dissertation (Northwestern University, 1974) (unpublished).
- <sup>26</sup>Values of the correlation energy from Refs. 9, 10, and 25 are those denoted by FSC(ANIS), i.e., "fully self-consistent and containing effects of anisotropy."
- <sup>27</sup>Eight-term polynomial fit to the correlation energy was also used and gave results essentially the same as that Wigner-like form (see text).
- <sup>28</sup>Values of  $D$  and  $E$  in the Wigner fit to the bulk correlation energies were obtained by a least-squares fit to the numerical results in Refs. 9, 10, and 25 in which values of the energy corresponding to densities in the region of one-half the bulk density were preferentially weighted because the region of these densities gives the largest contribution to the surface tension. This procedure gives values of the surface tension and critical temperature which differ by  $\leq 1\%$  from those obtained using an unweighted least-squares fit to the Wigner form.
- <sup>29</sup>T. M. Rice, *Nuovo Cimento B* 23, 226 (1974).
- <sup>30</sup>We take this opportunity to correct a numerical error in the temperature-dependent term in  $g_i$  given in Ref. 16. This change in  $g_i$  has been found to have only a very small effect on the resulting values of surface tension and critical temperature.
- <sup>31</sup>J. H. Rose and H. B. Shore, *Phys. Rev. B* 18, 1884 (1978).
- <sup>32</sup>B. Y. Tong and L. J. Sham, *Phys. Rev.* 144, 1 (1966).
- <sup>33</sup>J. Vannimenus and H. F. Budd, *Solid State Commun.* 15, 1739 (1974).
- <sup>34</sup>These values of  $\rho_0(0)$  and  $\delta_p$  were obtained by using the eight-term polynomial fit given in Ref. 35 to the correlation energy of Refs. 9, 10, and 25 rather than the Wigner fit in Eq. (7). This gives slightly more accurate values for  $\rho_0(0)$  and  $\delta_p$ .
- <sup>35</sup>R. K. Kalia and P. Vashishta, *Phys. Rev. B* 17, 2655 (1978).
- <sup>36</sup>Values given here for  $T_c$  for Ge[4;2] and Si[6;2] are somewhat larger than those given previously (Refs. 14 and 16) based on essentially the present method. We take this opportunity to point out that minor numerical error occurred in calculating  $\delta_\sigma$  previously and that those values of  $T_c$  for Ge[4;2] and Si[6;2] should have been essentially the same as the ones given in Table II.
- <sup>37</sup>We note that densities  $\rho \leq \frac{1}{2}\rho_0(0)$  give a somewhat larger contribution to the temperature-dependent term in  $\sigma(T)$  than  $\rho > \frac{1}{2}\rho_0(0)$ , hence the choice  $\bar{\rho} = 0.4\rho_0(0)$ .
- <sup>38</sup>In Ref. 16, the gradient contribution from the low-density tail region to the surface tension was treated by using an interpolation procedure between an expression appropriate for low density and that for high density. This procedure gives values consistent with the range of values quoted in the text.
- <sup>39</sup>T. L. Reinecke and S. C. Ying, *Solid State Commun.* 14, 381 (1974); T. L. Reinecke, F. Crowne and S. C. Ying, *Proceedings of the Twelfth International Conference on the Physics of Semiconductors, Stuttgart, 1974*, edited by M. H. Pilkuhn (Teubner, Stuttgart, 1974), p. 61.

- <sup>40</sup>In Refs. 14 and 16 we inadvertently quoted for  $\sigma(0)$  for Ge[4;2] the value  $2.70 \text{ K}/a_0^2$ ; the value should have been  $4.25 \text{ K}/a_0^2 = 0.688 \text{ a.u.}/a_0^2$  consistent with the results here.
- <sup>41</sup>Kalia and Vashishta (Ref. 35) have reported values for  $\sigma(0)$  for the six model systems studied here using a somewhat different method of calculation. Their values are consistently somewhat higher than those obtained here and in Ref. 31. We do not presently know the source of this difference.
- <sup>42</sup>L. M. Sander, H. B. Shore, and L. J. Sham, *Phys. Rev. Lett.* **31**, 533 (1973); T. M. Rice, *Phys. Rev. B* **9**, 1540 (1974); H. Büttner and E. Gerlach, *J. Phys. C* **4**, L433 (1973).
- <sup>43</sup>P. Vashishta, R. K. Kalia, and K. S. Singwi, *Solid State Commun.* **19**, 935 (1976); R. K. Kalia and P. Vashishta, *Solid State Commun.* **24**, 171 (1977).
- <sup>44</sup>M. Rasolt and D. J. W. Geldart, *Phys. Rev.* **15**, 979 (1977).
- <sup>45</sup>Phase diagrams are quite insensitive to the choice of  $\tau$ . We use  $\tau = 2.2$  from results for the lattice gas (Ref. 21).
- <sup>46</sup>R. N. Silver, *Phys. Rev. B* **11**, 1569 (1975); **12**, 5689 (1975).
- <sup>47</sup>R. M. Westervelt, *Phys. Status Solidi B* **74**, 727 (1976); **76**, 31 (1976).
- <sup>48</sup>For further discussion of the method, see T. L. Reinecke, *Phys. Rev. B* **16**, 2653 (1977).
- <sup>49</sup>Minor algebraic error has been corrected in the result from Ref. 46.
- <sup>50</sup>Values of the parameters used for the several systems are: for Ge [4;2],  $\phi/k_B = 23 \text{ K}$  (Ref. 51),  $\sigma(0) = 3.0 \times 10^{-4} \text{ erg/cm}^2$  (Refs. 31 and 47),  $\tau_0 = 40 \times 10^{-6} \text{ sec}$  (Ref. 52), and  $A = 8.2 \times 10^{20} \text{ sec}^{-1} \text{ cm}^{-2} \text{ K}^{-2}$ ; for Ge[1;1],  $\phi/k_B = 4.9 \text{ K}$  (Ref. 9),  $\sigma(0) = 0.2 \times 10^{-4} \text{ erg/cm}^2$  (text, Refs. 35, 41, 43, 48),  $\tau_0 = 400 \times 10^{-6} \text{ sec}$  (Ref. 53),  $A = 1.03 \times 10^{20} \text{ sec}^{-1} \text{ cm}^{-2} \text{ K}^{-2}$ ; for Si [6;2],  $\phi/k_B = 95 \text{ K}$  (Ref. 9),  $\sigma(0) = 85 \times 10^{-4} \text{ erg/cm}^2$  (text, Refs. 17, 35, and 54),  $\tau_0 = 0.2 \times 10^{-6} \text{ sec}$  (Ref. 53),  $A = 22.0 \times 10^{20} \text{ sec}^{-1} \text{ cm}^{-2} \text{ K}^{-2}$ ; for Si [2;1],  $\phi/k_B = 21.8 \text{ K}$  (Ref. 9),  $\sigma(0) = 8 \times 10^{-4} \text{ erg/cm}^2$  (text, Refs. 35 and 43),  $\tau_0 = 2 \times 10^{-6} \text{ sec}$ ,  $A = 3.67 \times 10^{20} \text{ sec}^{-1} \text{ cm}^{-2} \text{ K}^{-2}$ . The value of  $(\mu_G - \mu_I)/k_B T$  is relatively insensitive to  $\sigma(0)$ ,  $\tau_0$ , and  $A$ , values of which for some systems are not known accurately, and it is more sensitive to  $\phi$  which are known better. The value of  $A$  for Ge[4;2] was obtained from the data of Ref. 52, and the values for the other cases were obtained by adjusting this value according to the changing exciton mass and degeneracy.
- <sup>51</sup>T. K. Lo, *Solid State Commun.* **15**, 1231 (1974).
- <sup>52</sup>R. M. Westervelt, T. K. Lo, J. L. Stalhli, and C. D. Jeffries, *Phys. Rev. Lett.* **32**, 1051 (1974); **32**, 1331 (1974).
- <sup>53</sup>Ya. E. Pokrovsky, *Phys. Status Solidi A* **11**, 385 (1972).
- <sup>54</sup>J. Collet, M. Pugno, J. Barrau, M. Brousseau, and H. Maaref, *Solid State Commun.* **24**, 375 (1977).
- <sup>55</sup>J. Shah, M. Combescot, and A. H. Dayem, *Phys. Rev. Lett.* **38**, 1497 (1977).
- <sup>56</sup>A. Forchel and W. Schmid (unpublished).
- <sup>57</sup>A. F. Dite, V. D. Kulakovskii, and V. B. Timofeer, *Sov. Phys. JETP* **45**, 604 (1977).
- <sup>58</sup>W. Miniscalco, C.-C. Huang, and M. B. Salamon, *Phys. Rev. Lett.* **39**, 1356 (1977).
- <sup>59</sup>This can be seen, for example, by comparing the bulk exchange plus correlation energies for the six model systems studied here from the calculations of Refs. 9, 10, and 25.
- <sup>60</sup>T. L. Reinecke and S. C. Ying (unpublished).
- <sup>61</sup>See also a comment made by H. L. Störmer, R. W. Martin, and J. C. Hensel, *Proceedings of the Thirteenth International Conference on the Physics of Semiconductors, Rome, 1976*, edited by F. G. Fumi (Tipografia, Marves, Rome, 1977), p. 950.
- <sup>62</sup>In Fig. 4(a) data from Thomas *et al.*, Ref. 12, which does not include the recent reanalysis of the data for the gas side of the phase diagram by these authors (Ref. 22), is shown.
- <sup>63</sup>Values of the parameters used are: for Ge[4;2],  $\rho_0(0) = 2.38 \times 10^{17} \text{ cm}^{-3}$ ,  $\delta_p = 0.0092 \text{ K}^{-2}$ , and  $T_c = 6.5 \text{ K}$ ; for Si[6;2],  $\rho_0(0) = 3.3 \times 10^{18} \text{ cm}^{-3}$ ,  $\delta_p = 0.000450 \text{ K}^{-2}$ , and  $T_c = 27 \text{ K}$ .
- <sup>64</sup>R. M. Westervelt, J. L. Staehli, E. E. Haller, and C. D. Jeffries, *Proceedings of the Oji Seminar on Physics of Highly Excited States in Solids, Tomakomai, 1975*, edited by M. Ueta and Y. Nishina (Springer, Berlin, 1976), p. 270.
- <sup>65</sup>B. Etienne, C. Benoit à la Guillaume, and M. Voos, *Phys. Rev. B* **14**, 712 (1976).
- <sup>66</sup>J. L. Staehli, *Phys. Status Solidi B* **75**, 451 (1976).
- <sup>67</sup>B. Etienne, L. M. Sander, C. Benoit à la Guillaume, M. Voos, and J. Y. Prieur, *Phys. Rev. Lett.* **37**, 1299 (1976).
- <sup>68</sup>M. Combescot, *Phys. Rev. Lett.* **32**, 15 (1974).
- <sup>69</sup>In Ref. 10 the authors apparently inadvertently used an incorrect density dependence for the chemical potential.
- <sup>70</sup>T. M. Rice, *Proceedings of the Twelfth International Conference on the Physics of Semiconductors, Stuttgart, 1974*, edited by M. H. Pilkuhn (B. G. Teubner, Stuttgart, 1974), p. 23; T. M. Rice, Ref. 2.
- <sup>71</sup>See, e.g., M. E. Fisher, *Phys. Rev.* **162**, 480 (1967); C. J. Thompson, *Commun. Math. Phys.* **24**, 6 (1971).
- <sup>72</sup>Mahler and Birman (Ref. 15) have made a somewhat similar point based on a rather different argument.